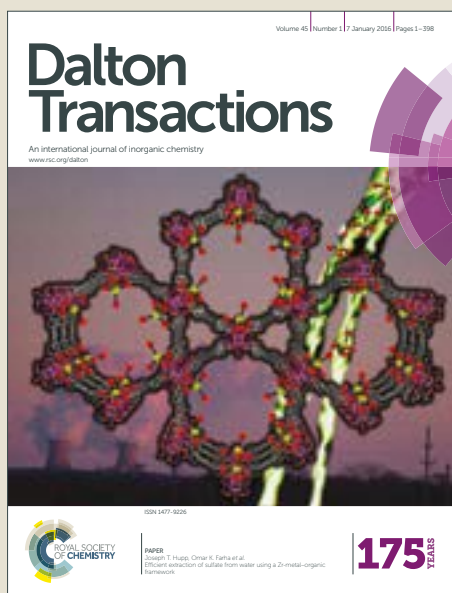


# Dalton Transactions

Accepted Manuscript



This article can be cited before page numbers have been issued, to do this please use: H. Kaur, M. Venkateswarulu, S. Kumar, V. Krishnan and R. R. Koner, *Dalton Trans.*, 2017, DOI: 10.1039/C7DT04057A.



This is an Accepted Manuscript, which has been through the Royal Society of Chemistry peer review process and has been accepted for publication.

Accepted Manuscripts are published online shortly after acceptance, before technical editing, formatting and proof reading. Using this free service, authors can make their results available to the community, in citable form, before we publish the edited article. We will replace this Accepted Manuscript with the edited and formatted Advance Article as soon as it is available.

You can find more information about Accepted Manuscripts in the [author guidelines](#).

Please note that technical editing may introduce minor changes to the text and/or graphics, which may alter content. The journal's standard [Terms & Conditions](#) and the ethical guidelines, outlined in our [author and reviewer resource centre](#), still apply. In no event shall the Royal Society of Chemistry be held responsible for any errors or omissions in this Accepted Manuscript or any consequences arising from the use of any information it contains.



## Dalton Transactions

## PAPER

## Metal-organic framework based multifunctional catalytic platform for organic transformation and environmental remediation

Harpreet Kaur,<sup>a</sup> M. Venkateswarulu,<sup>a</sup> Suneel Kumar,<sup>a</sup> Venkata Krishnan<sup>a</sup> and Rik Rani Koner<sup>\*b</sup>

Received 00th January 20xx,  
Accepted 00th January 20xx

DOI: 10.1039/x0xx00000x

[www.rsc.org/](http://www.rsc.org/)

Given the need of efficient reaction platform, a multifunctional material has been developed through integration of iodine into a Cd<sup>2+</sup> based MOF as a new catalytic system for organic transformation. Further, the Cd-MOF itself has been successfully used as potential material for photocatalytic dye degradation. The iodine incorporated MOF showed tremendous efficiency in the organic catalysis for the synthesis of a library of benzimidazole derivatives with yield > 80%. In addition, the same iodine loaded MOF (I<sub>2</sub>@Cd-MOF) exhibits good applicability and reusability for the synthesis of thienyldipyrromethane. Apart from this, the photocatalytic activity of Cd-MOF was also evaluated under visible light irradiation which revealed excellent photocatalytic activity (82%) for MB degradation without the use of any enhancer. Altogether, this catalytic platform established its efficacy as a multifunctional catalyst in organic synthesis of biologically active motifs and photocatalytic dye degradation.

### Introduction

In recent times, there is great demand for developing multifunctional materials for several practical applications. Among the various kinds of materials, metal organic frameworks (MOFs) have been found to be promising materials due to their vast applications such as gas storage and separation, drug delivery, sensing, magnetism, nonlinear optics, luminescence, proton conduction and energy storage etc.<sup>1-7</sup> MOF derived hybrid materials have also attracted immense attention particularly in asymmetric catalysis, organic catalysis, electrocatalysis and photocatalysis in comparison to other porous materials.<sup>8-12</sup> The open metal centres of MOF materials offer an active reaction sites as well as tunable porosity with large surface area, which allow the substrates and guest species to get into the channels and access the internal reaction center.<sup>13</sup>

Although, a number of catalytic MOFs and iodine loaded MOFs have already been developed and reported,<sup>14-15</sup> MOFs as a multifunctional catalytic platform has not been explored in detail.<sup>2b</sup> The heterogroup functionalized linkers based MOFs have been preferred for better catalytic activity and particularly MOFs with amino functionalized linkers already exhibited better catalytic activity compared to non-functionalized MOF. This inspired us to

select an innovatively designed and developed Cd-MOF based on amino functionalized terephthalic acid and 4,4'-bipyridine linker.<sup>5</sup> We have explored the functional Cd-MOF for the development of a new MOF-iodine integrated catalytic system for various organic transformations as well as for the photocatalytic degradation of a model pollutant (Scheme 1 and S1). In order to investigate its catalytic applicability and to understand the releasing profile of iodine, we have chosen different organic reactions which resulted into biologically active products.

After detailed characterization of iodine incorporation, we employed I<sub>2</sub>@Cd-MOF for the synthesis of benzimidazole derivatives, known for pharmacological activity, catalysis and various other applications.<sup>16-18</sup> Although synthetic procedures employing simple molecular I<sub>2</sub> as a catalyst have also been reported earlier,<sup>19</sup> the drawbacks have been the high reaction temperature, longer reaction time and low yield. Successful iodine incorporation enabled us to improve reaction time substantially (4 times lower) along with considerable enhancement in reaction yield as compared to reaction in the presence of iodine alone. In addition, we have also employed this I<sub>2</sub>@Cd-MOF for the synthesis of thienyldipyrromethane which pronounced to be the important precursor in the synthesis of porphyrin and boron-dipyrromethanes (BODIPY) analogs.<sup>20-22</sup>

Apart from the organic catalysis, we have also explored the potential of this Cd-MOF for photocatalytic degradation of methylene blue (MB) efficiently. Methylene Blue is one of the widely used well known dye in various fields and, the non-degradation nature of MB makes serious impact on environment. Even a small amount of MB causes harmful effects which includes

<sup>a</sup> School of Basic Sciences, Indian Institute of Technology Mandi, Mandi-175001, H.P., India.

<sup>b</sup> School of Engineering, Indian Institute of Mandi, Mandi-175001, H.P., India.

<sup>c</sup> Email- rik@iitmandi.ac.in, Fax: +91 1905 237924; Tel: +91 1905 267220.

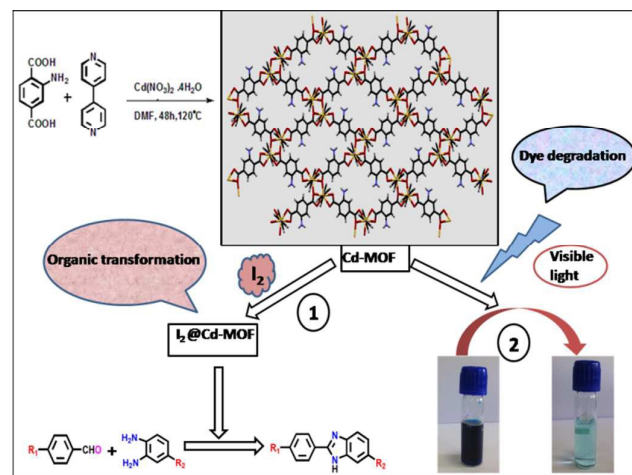
Electronic Supplementary Information (ESI) available: [details of any supplementary information available should be included here]. See DOI: 10.1039/x0xx00000x

## PAPER

## Dalton Trans.

haemolytic anemia in infants, vomiting, chest pain, fever, hypotension and bluish discoloration of skin.<sup>23-24</sup>

Given the adverse effect of MB, the amino functionalized Cd-MOF was employed for the degradation of MB to evaluate its photocatalytic efficiency. This MOF exhibited very high efficiency in the catalytic degradation of MB without the use of any photocatalytic enhancers such as H<sub>2</sub>O<sub>2</sub>, KBrO<sub>3</sub>, RGO etc.



**Scheme 1** Schematic pathway of Cd-MOF for photocatalysis and organic transformation.

## Experimental Section

### Materials and Methods

Cadmium nitrate, 4,4'-bipyridine, 2-aminoterephthalic acid, DMF were purchased from Alpha Aesar. All reagents and solvents were used as such without any further purification. TGA was performed on Perkin Elmer Analyzer under nitrogen with heating rate of 10°C/min from 30 to 800°C. Powder X-ray diffraction measurements were done using an Aligent Supernova X-Ray Diffractometer using Cu-K $\alpha$  radiations at 45 kV and 40 mA with 2 $\theta$  value ranging from 5° to 80° with scan rate of 2°/min and scan step of 0.02°. Perkin Elmer spectrum 2 spectrophotometer was used for recording FT-IR spectra. Jeol ECX-500MHz spectrometer (internal standard: TMS) was used for recording <sup>1</sup>H and <sup>13</sup>C-NMR spectra in DMSO-*d*<sub>6</sub>. The absorption spectra was measured using SHIMADZU UV-2450 spectrophotometer. The morphology was measured on FEI Nova Nano SEM-450, field emission scanning electron microscopy (FE-SEM) and a high resolution transmission electron microscope (HRTEM) FEI Tecnai G2 20 S-twin microscope with operating voltage of 200kV. Energy dispersive X-ray spectra (EDAX) were also obtained using the same instrument. X-ray photoelectron spectroscopic (XPS) measurements were done with the use of SCIENTA, R-3000 analyzer with dual anode Al k $\alpha$  (1486.6 eV) as a source operating at anode voltage of 12 kV and filament current of 23 mA. The data obtained from the instrument was solved with the help of CASA software. N<sub>2</sub> adsorption isotherms and BET surface

areas were measured by using Quantachrome Autosorb-iQ-MP-XR system at 77K.

### Single crystal X-ray diffraction studies

Crystals of Cd-MOF were grown by solvothermal method for single crystal X-ray diffraction analysis. The data were collected using CrysAlis Pro Software (online version) and CrysAlisPro Software (offline version) was used for data reduction. Olex2 and SHELXS (1, 2) direct methods were used to solve the structure of Cd-MOF. Full-matrix least squares on F<sub>2</sub> were used to refine the data.

### Synthesis of Cd-MOF(C<sub>18</sub>H<sub>8</sub>CdN<sub>3</sub>O<sub>4</sub>)

Cd-MOF was synthesized following the reported procedure with slight modifications (Scheme 1 and S1).<sup>5</sup> Cd(NO<sub>3</sub>)<sub>2</sub>·6H<sub>2</sub>O (0.156g, 1mmol), 4,4'-bipyridine (0.075g, 1mmol), 2-aminoterephthalic acid (0.030g, 1mmol) and DMF (3 mL) were mixed and sealed in a 25 mL Teflon lined acid digestion bomb, then placed inside oven followed by heating at 120 °C for 2 days. After cooling to room temperature, the rod shape crystals were obtained by filtration, then washed with DMF/Ethanol (1:1) mixture (5mL). Finally, crystals were dried under vacuum for 24h. Yield: 68.8%. FT-IR (KBr,  $\nu$  in cm<sup>-1</sup>): 3331, 2402, 1660, 1535, 1527, 1392, 1254, 1218, 1157, 848, 780.

### Iodine adsorption and desorption

Iodine adsorption study was performed by immersing 100mg of Cd-MOF crystals to 5 mL of 0.1 M hexane solution of iodine in a glass vial.<sup>25</sup> The colour of the iodine solution gradually started diminishing which indicated the adsorption of iodine over MOF within 5 h (Fig. 1). Further, the solution was filtered and the crystals were given washings with fresh hexane solution (4-5 times) to remove free iodine present at the crystals surface. Next iodine loaded MOF crystals (I<sub>2</sub>@Cd-MOF) were obtained by air drying at room temp (Fig. S2). Furthermore, the desorption of iodine loaded in MOF was also performed by immersing it in ethanol for 24h (Fig.S3).

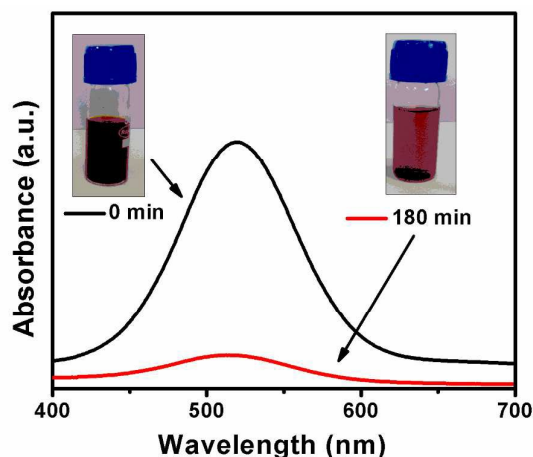


**Fig.1** UV-vis spectra of 0.1M hexane solution of iodine at 0 min and 180 min respectively.

### Catalytic performance

The I<sub>2</sub>@Cd-MOF was explored as efficient catalyst toward the synthesis of benzimidazole derivatives from substituted benzaldehydes and o-phenylenediamines using I<sub>2</sub>@Cd-MOF as well as the synthesis of thienyl dipyrromethane derivative.

#### General Procedure

**2-phenyl-1H-benzo[d]imidazole (1a):** Benzaldehyde (0.106g, 1 mmol), o-phenylenediamine (0.108g, 1mmol), I<sub>2</sub>@Cd-MOF (0.150g, 33mmol%) and Na<sub>2</sub>SO<sub>4</sub> (5mmol) were mixed in DMSO (5mL) and stirred at room temperature. Reaction progress was monitored by TLC. After the completion of the reaction (6h) the mixture was diluted with DCM and then filtered to separate the catalyst. To this filtrate, saturated aqueous solution of Na<sub>2</sub>S<sub>2</sub>O<sub>3</sub> was added to remove the coloration due to iodine. Then the reaction mixture was extracted with DCM:H<sub>2</sub>O (3 times). The extract was then washed with brine, dried over Na<sub>2</sub>SO<sub>4</sub> and evaporated to obtain the product. Yield: 85%. <sup>1</sup>H-NMR (500MHz, DMSO-*d*<sub>6</sub>) δ: 7.29(m, 2H), 6.80-6.69(m, 5H), 6.4(m, 2H) ppm. HRMS: (m/z) calculated for C<sub>13</sub>H<sub>11</sub>N<sub>2</sub> [M+1] 195.0922 found 195.0916. The recovered catalyst was dried and used further for the next cycle.

**6-methyl-2-phenyl-1H-benzo[d]imidazole (1b):** This was synthesized from benzaldehyde (0.106g, 1mmol) and 4-methylbenzene-1,2-diamine (0.134g, 1mmol) using the same procedure like **1a** and purified by column chromatography with MeOH/DCM (.5%). Yield: 75%. <sup>1</sup>H-NMR (500MHz, DMSO-*d*<sub>6</sub>) δ: 12.7(bs, 1H), 8.15(d, 2H), 7.56-7.45(m, 4H), 7.37(s, 1H), 7.02(d, 1H), 2.42(s, 3H) ppm. HRMS: (m/z) calculated for C<sub>14</sub>H<sub>12</sub>N<sub>2</sub>[M+1] 209.1079 found 209.1236.

**phenyl(2-phenyl-1H-benzo[d]imidazol-5-yl)methanone (1c):** This was synthesized from benzaldehyde (0.106g, 1mmol) and 3,4-diaminophenyl(phenyl)methanone (0.233g, 1.1mmol) following procedure of **1b**. Yield: 70%. <sup>1</sup>H-NMR (500MHz, DMSO-*d*<sub>6</sub>) δ: 13.2(bs, 1H), 8.2(d, 1H), 7.7(m, 2H), 7.5(m, 5H), 7.4(m, 2H), 7.07(d, 1H), 6.8(m, 1H), 6.5(d, 1H) ppm. HRMS: (m/z) calculated for C<sub>20</sub>H<sub>15</sub>N<sub>2</sub>O [M+1] 299.1184 found 299.1276.

**2-(4-fluorophenyl)-1H-benzo[d]imidazole (1d):** This was synthesised from 4-fluorobenzaldehyde (0.068g, 1.1mmol) and o-phenylenediamine (0.108g, 1mmol) following procedure of **1b**. Yield: 70%. <sup>1</sup>H-NMR (500MHz, DMSO-*d*<sub>6</sub>) δ: 12.9(bs, 1H), 8.24-8.19(m, 2H), 7.53(m, 2H), 7.42-7.37(m, 2H), 7.23-7.17(m, 2H) ppm. HRMS: (m/z) calculated for C<sub>13</sub>H<sub>8</sub>N<sub>2</sub>F [M-1] 211.0672 found 211.0664.

**2-(4-bromophenyl)-1H-benzo[d]imidazole (1e):** This was synthesised from 4-bromobenzaldehyde (0.101g, 1.1mmol) and o-phenylenediamine (0.108g, 1mmol) following procedure of **1b**. Yield: 70%. <sup>1</sup>H-NMR (500MHz, DMSO-*d*<sub>6</sub>) δ: 13.01(bs, 1H), 8.12(d, 2H), 7.76(d, 2H), 7.67(d, 2H), 7.53(d, 1H), 7.24-7.17(m, 2H) ppm. HRMS: (m/z) calculated for C<sub>13</sub>H<sub>11</sub>N<sub>2</sub>Br [M+1] 273.0027 found 273.0120.

**4-(1H-benzo[d]imidazol-2-yl)-N,N-dimethylbenzenamine (1f):** This was synthesised using 4-(dimethylamino)benzaldehyde (0.164g, 1.1mmol) and o-phenylenediamine (0.108g, 1mmol) following above procedure of **1b**. Yield: 73%. <sup>1</sup>H-NMR (500MHz, DMSO-*d*<sub>6</sub>) δ: 13.01(bs, 1H), 7.69(d, 2H), 6.99(m, 2H), 6.76 (d, 2H), 6.66(d, 2H),

3.04(s, 6H) ppm. HRMS: (m/z) calculated for C<sub>15</sub>H<sub>15</sub>N<sub>3</sub> [M+1] 238.1300 found 238.1355.

**5-(2-thienyl)dipyrromethane (2a):** Thiophene-2-carboxaldehyde (0.200g, 1mmol), pyrrole (0.300g, 5mmol) and I<sub>2</sub>@Cd-MOF (0.030g) were mixed and stirred at room temperature. The reaction progress was monitored by TLC. The reaction color became green after some time and changes to somewhat red which indicates the completion of the reaction. After 5 h, 5 mL of dichloromethane was added to the reaction mixture and then filtered. The filtrate was treated with 5 mL of water three times and then dried over anhydrous Na<sub>2</sub>SO<sub>4</sub>. The obtained viscous red compound was purified by column chromatography (1:1 ratio of hexane and dichloromethane mixture). Yield: 68%.

<sup>1</sup>H-NMR(500MHz, DMSO-*d*<sub>6</sub>) δ: 8.06(bs, 2H), 7.2(m, 1H), 6.89-6.95(m, 1H), 6.81(d, 1H), 6.69(m, 2H), 6.16(m, 2H), 6.04(m, 2H), 5.7(s, 2H) ppm. HRMS: (m/z) calculated for C<sub>13</sub>H<sub>13</sub>N<sub>2</sub>S [M-1] 229.0769 found 229.0569.

#### Photocatalytic Dye Degradation

The photocatalytic activity of Cd-MOF was studied by performing the photocatalytic degradation of MB dye by illuminating under visible light at room temperature and pressure using a home built photocatalytic reactor equipped with visible light source.<sup>26</sup> Typically, photocatalyst Cd-MOF (40 mg) was dispersed in 100 mL of 5 × 10<sup>-5</sup>M (0.0159L<sup>-1</sup>) aqueous solution of MB. Before irradiation, the resultant solution was stirred magnetically in dark for 30 min to obtain the adsorption-desorption equilibrium in between the dye and the photocatalyst. As the equilibrium was set up, the suspension was illuminated under visible light. After each 15 min, 1 mL of the sample solution was collected, centrifuged and transferred for UV-analysis. Simultaneously, the same set of experiment was carried out without any MOF catalyst to monitor the self-photosensitization of MB. In addition, same experiment with Cd-MOF catalyst was performed in dark (in the absence of visible light) to confirm whether there is any adsorption of dye molecules by Cd-MOF.

## Results and Discussion

#### Crystal Structure

The single crystal of Cd-MOF was synthesized from the reported hydrothermal method with slight modifications (Fig S1). The single crystal of Cd-MOF was grown in an orthorhombic crystal system with P2<sub>1</sub>2<sub>1</sub>2 space group. The crystallographic data collection parameters and data refinement details of Cd-MOF are summarized in Table S1. Fig. 2a showed the ball and stick model view of the asymmetric unit of Cd-MOF and its ellipsoid model with 50% probability level. The single crystal data revealed that the coordination environment of cadmium ion is satisfied by three different 2-ATC (2-amino terephthalic acid) ligands on the equatorial positions where as the two axial positions were occupied by 4,4'-bpy (bipyridine) units. Here, one of the carboxyl unit of 2-ATC acts as a chelating unit (η<sup>2</sup> mode) while the other one plays as a chelating bridging unit (μ<sub>2</sub>-η<sup>2</sup>; η<sup>1</sup> mode).<sup>27</sup> In crystal lattice, the central metal ion, Cd(II) is surrounded by pillar and planar

## PAPER

## Dalton Trans.

connectors like Bpy and 2-ATC units respectively. Finally, these connectivity and interactions lead to form the 3D 2-fold interpenetrated network of Cd-MOF (Fig. 2c).

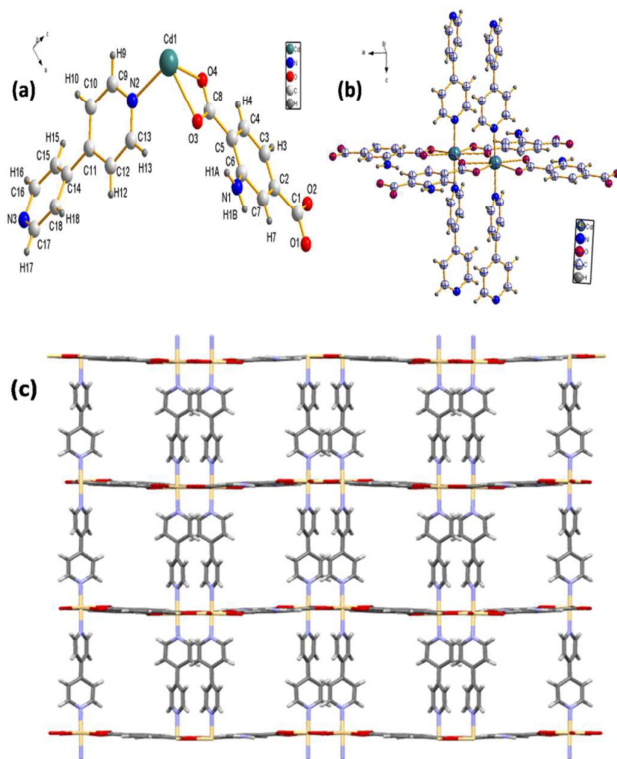


**Fig.2** (a) Asymmetric unit of Cd-MOF along with numbering scheme. (b) ORTEP modal view of cadmium complex. Thermal ellipsoids are scaled to the 50% probability level. (c) View of 3D network of Cd-MOF along b-axis.

### Thermal and Morphological studies

The thermal stability of the Cd-MOF was investigated using thermogravimetric analysis (TGA) and found to be stable upto 400°C. After that, continues weight loss was observed upto 550°C due to ligands decomposition (Fig.3). The iodine uptake capacity of Cd-MOF was also measured by thermogravimetric analysis which revealed that MOF is able to uptake 23 wt% of iodine (adsorption (Fig.3)). The accumulation of large amount of iodine within MOF framework is attributed to the charge transfer complex through weak interactions between iodine and NH<sub>2</sub> group of the linker moiety.<sup>23</sup> The TGA was performed before and after iodine loading. The amount of iodine released during each cycle of organic transformation was also determined by TGA study. The scanning electron microscopy (SEM) and transmission electron microscopy (TEM) images showed the rod shape morphology of MOF with stacked layers (Fig. S4a, b and S6a), whereas I<sub>2</sub> molecules spread over the surface of MOF (Fig. S4 c,d and S6b) in iodine-MOF

composite. The presence of iodine was further confirmed by energy dispersive X-ray spectroscopy (Fig. S5b and S7b).

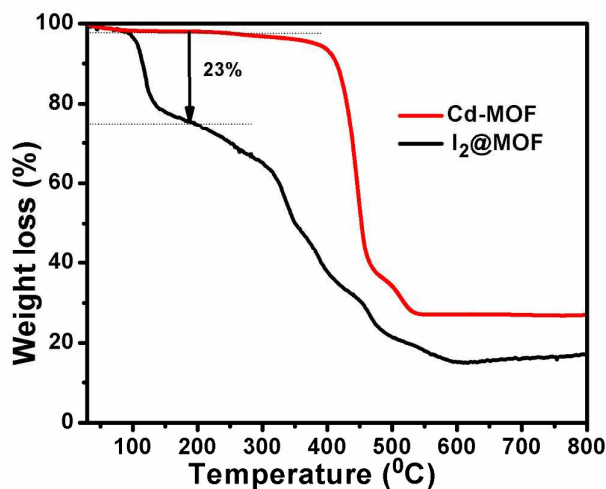


**Fig.3** TGA of Cd-MOF and I<sub>2</sub>@ Cd-MOF.

### Iodine adsorption studies

The adsorption-desorption studies of iodine revealed the iodine capturing behaviour of the Cd MOF.<sup>14a,25</sup> The time dependent UV-vis experiment was studied and found that upon addition of MOF crystals, the concentration of iodine in hexane solution got decreased from 1.41 a.u. to 0.11 a.u. within 180 min (Fig. S8). The slow desorption rate was confirmed by immersing the iodine loaded MOF crystals in ethanol. The result showed the change in color of ethanol with time due to iodine release into ethanol solution from I<sub>2</sub>@Cd-MOF crystals (Fig.S9). The color change was observed upto 24 h and it changed slowly from colorless to brown. The slow release of iodine tempted us to check the catalytic behaviour of I<sub>2</sub>@MOF.

### Catalytic transformation study

In an attempt to initiate our study, first reaction was carried out between benzaldehyde (1 mmol) and o-phenylenediamine (1 mmol), using I<sub>2</sub>@Cd-MOF as a catalyst for synthesizing benzimidazole derivatives (Scheme 2). Generally, molecular I<sub>2</sub> acts as a homogeneous catalyst and is used widely for the catalysis of various organic transformations,<sup>28,29,30</sup> whereas in the case of I<sub>2</sub>@Cd-MOF, the weak host guest interactions are mainly responsible for the stabilization of iodine species in the framework pores, which can be readily used for the catalysis and gives better yield. The existence of iodine as I<sub>2</sub> (in 0 oxidation state) within the pores was verified by the XPS studies (Fig.4).<sup>14a,31</sup> This was further supported by N<sub>2</sub> adsorption studies. Cd-MOF and I<sub>2</sub>@Cd-MOF showed N<sub>2</sub> uptake value of 17.186 cm<sup>3</sup>/g and 7.549 cm<sup>3</sup>/g at 77 K respectively (Fig. S10). The reduced N<sub>2</sub> uptake for iodine loaded MOF may be attributed to the adsorbed iodine which affects the passage of N<sub>2</sub> gas molecules into the channel pores.

A series of test reactions were carried out for optimizing the best reaction conditions. Initially, the reaction was performed with

aldehyde and diamine keeping the ratio 1: 1.5 and using t-BuOH as a solvent,<sup>32</sup> but the yield turned out to be very low~ 20%. The low

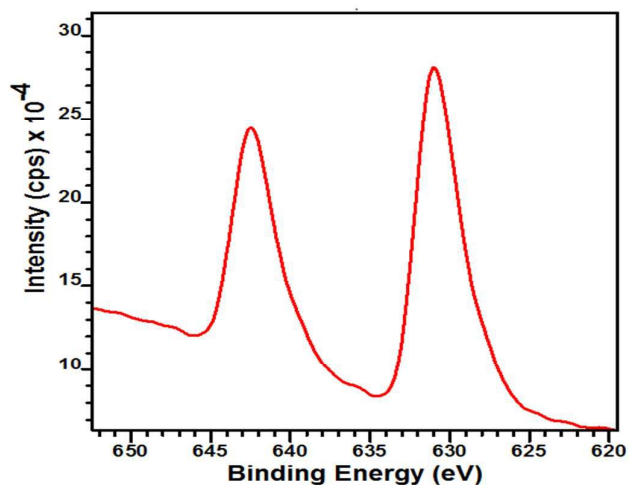


Fig.4 XPS spectrum of I<sub>2</sub>@Cd-MOF

yield of product may be attributed to the excess of diamine and lesser amount of catalyst. The yield of the product got increased after several optimizations such as by varying the molar ratio of aldehyde and diamine and amount of catalyst. But in these cases, the efficiency in terms of reaction progress time and yield was not much higher than that in the case of simple molecular I<sub>2</sub> using same solvent. To improve the yield, the effect of solvent was also studied and noticed appreciable improvement in yield in the presence of DMSO solvent. Further to investigate the required catalyst amount for better efficiency of the reaction, the reaction was performed under different catalytic ratio and observed that best results were obtained with 33mmol % of catalyst (Table 1).



Scheme2 Synthesis of Benzimidazole derivatives from benzaldehyde and o-phenylenediamine.

Table 1 Optimization of catalyst ratio required for better yield.

Catalyst	Catalyst ratio (mmol %)	% Yield
Iodine loaded Cd-MOF (t-BuOH as a solvent)	10	40
	15	50
	20	65
	33	70

Finally, we could able to isolate the product with 85% yield within 6h using 33 mmol% of catalyst in the presence of DMSO as solvent. On contrary, the same reaction took 24h to produce 70% yield at high temperature in the presence of molecular I<sub>2</sub>.<sup>19</sup> This indicated that, I<sub>2</sub>@Cd-MOF played as superior and efficient catalyst than molecular I<sub>2</sub>. The accessible functionalized surface area of iodine

integrated MOF system induced the reactant which led to increase the reaction rate and yield of the product. After optimizing the reaction conditions, reaction scope was expanded by performing

Table 2 Synthesis of benzimidazoles from substituted benzaldehydes and diamines catalysed by I<sub>2</sub>@Cd-MOF.

S. No.	Benzaldehyde	Diamines	Product	No	% Yield
1				1a	85
2				1b	75
3				1c	70
4				1d	70
5				1e	70
6				1f	73

Conditions: a. Room temperature, b. Drying agent: Na<sub>2</sub>SO<sub>4</sub>, c. Solvent: DMSO, d. Time: 6h

the reaction with different aldehyde and diamine derivatives bearing both electron withdrawing and releasing group. The effect of electronic parameter was evident from the reaction yield (Table 2) (Fig. S11-S22).

Next, the reusability of the catalyst, the most important part in catalysis reaction from economic point of view was also examined. The catalyst was recovered either by centrifugation or filtration from the reaction mixture and allowed to be used for the next cycle. However, the yield in the second cycle turned upto 62% due to less amount of iodine available in I<sub>2</sub>@Cd-MOF. The amount of iodine released in both the cycles was estimated by TGA (Fig. 5). In the first cycle, 11% of iodine got released into reaction mixture and in second cycle, the amount of iodine released was 4%.

In addition to make sure the reusability of this I<sub>2</sub>@MOF, one more organic transformation was performed. We chose a known organic transformations i.e the synthesis of 5(2-thienyl) dipyrromethane<sup>10b</sup> (Scheme 3) (Fig. S23-S24). As our attempt was to explore the reusability of I<sub>2</sub>@MOF, the reaction was performed under similar

reported condition.<sup>25</sup> In the synthesis of 5(2-thienyl)dipyrromethane, the catalyst was found to be efficient and recyclable. Thermogravimetric analysis revealed the slow release of iodine during catalytic reactions which led to perform consecutive three cycles of this reaction. In first cycle about 9% of iodine was released whereas in the next two cycles the amount of iodine released was 7% and 6%, which can be seen from the TGA curves

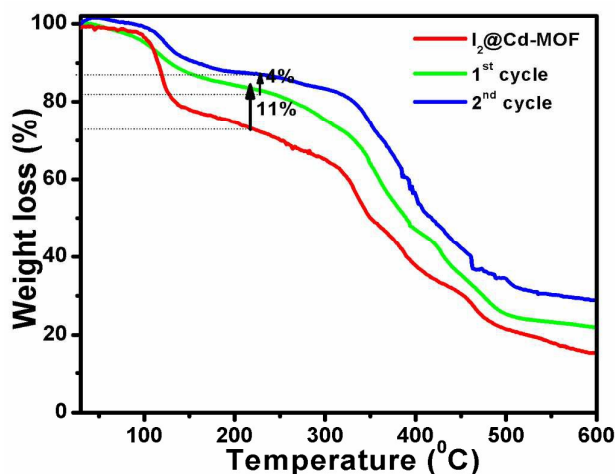
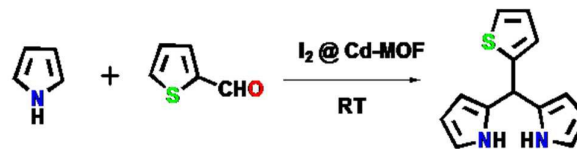


Fig. 5 TGA graph for iodine releasing profile during synthesis of 2-phenyl-1H-benzo[d]imidazole.

(Fig. S25a). The reaction time for each cycle was kept constant. The yield of the product after each cycle got diminished due to the less availability of iodine (Fig. S25a).

This was further being supported by TEM- EDAX data of MOF recovered after reaction (Fig. S26a and b). Further, to check the stability of Cd-MOF, PXRD analysis were carried out for I<sub>2</sub>@Cd-MOF before and after organic catalysis, which revealed similar pattern as that of pure Cd-MOF (Fig. S27a,c and d).



Scheme 3 Synthesis of thienyl dipyrromethanes.

### Photocatalytic Studies

#### Optical Band Gap

In order to investigate the conductivity of Cd-MOF, the diffuse reflectance spectroscopy (DRS) was performed in the range of 200–800 nm to determine the band gap ( $E_g$ ). From DRS spectra, it can be clearly seen that Cd-MOF has an absorption edge at 442nm (Fig. S28) which corresponds to a band gap of 2.8eV. Thus the  $E_g$  value clearly imparts for the Cd-MOF absorption in the visible region which constitutes a major part of sunlight.

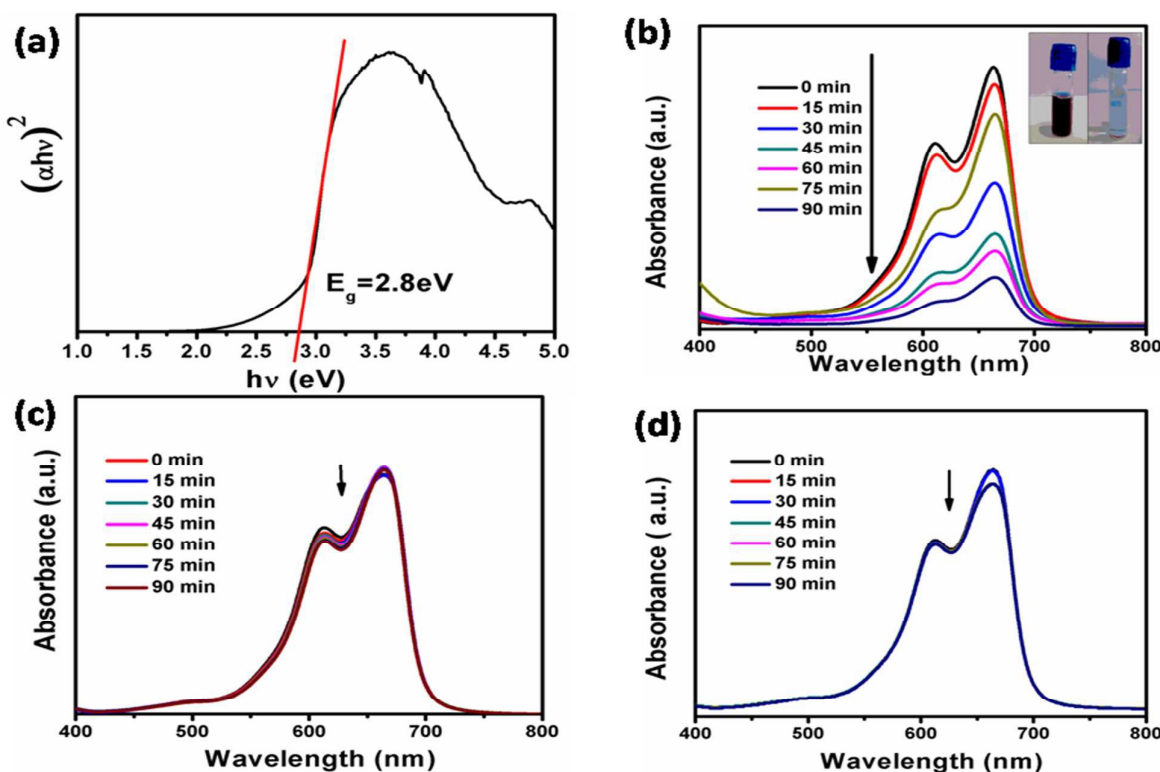


Fig. 6(a) Plot showing transformed Kubelka- Munk function vs. energy of light for band gap. Photocatalytic degradation of MB under visible light irradiation: (b) in the presence of catalyst. (c) in the absence of catalyst and (d) Degradation of MB with catalyst in dark.

## Dalton Transactions

## PAPER

The  $E_g$  value was calculated from a plot of Kubelka-Munk function  $F$  versus energy (Fig. 6a). It has been found that the band gap of this particular Cd-MOF is relatively lower than other reported MOFs and typical inorganic wide band gap semiconductor materials.<sup>33,34,35</sup>

## Study of Photocatalytic activity

The photocatalytic degradation of MB was studied under visible light irradiation to examine the photocatalytic efficiency of Cd-MOF. The characteristic absorption peak of MB gradually decreased with increase in exposure time in the presence of Cd-MOF catalyst (Fig. 6b). Whereas, the absorbance intensity of MB was remained

it confirmed that there is no adsorption and it was completely a degradation process. This was also confirmed by TEM-EDAX data of Cd-MOF recovered after photocatalytic dye degradation, in which sulphur content was found to be zero (Fig. S29a and b). Notably, the Cd-MOF showed excellent photocatalytic activity with 82% MB degradation within 90 min in visible region without the addition of any photocatalytic enhancers like reduced graphene oxide,  $\text{KBrO}_3$ ,  $\text{H}_2\text{O}_2$ . Apart from visible light irradiation, the efficiency of Cd-MOF was also examined under UV light. Under UV light irradiation, the catalyst showed only 72% degradation of MB dye in same time period of 90 minutes which can be clearly justified from the fact that Cd-MOF is visible light active (Fig. S30d).

The degradation rate was calculated as the kinetic data of the MB degradation well fitted with pseudo 1st order kinetics (Fig. 7a and b).<sup>23,36</sup>

The degradation rate can be calculated using the following equation<sup>37</sup>:

$$\% \text{ Degradation} = (1 - A_t / A_0) \times 100$$

Where  $A_t$  and  $A_0$  are the absorbance at the time  $t$  and initial absorbance respectively, which corresponds to relative concentrations.

The better photocatalytic activity of Cd-MOF may be attributed to the interaction of  $\text{NH}_2$  group of linker moiety towards MB, which is the governing factor for adsorbing MB over MOF surface. The Cd-MOF established its efficiency towards the photocatalytic degradation of MB dye than many other reported MOFs (Table S2).<sup>38-42</sup>

Next, the stability of Cd-MOF was studied by checking its reusability for photocatalytic degradation of MB dye. In this case, four cycles of degradation experiments were performed by recovering the catalyst each time after completion the process (Fig. S30a to c). The recyclability results are shown in Fig. 8. It can be clearly seen that the catalyst showed good photocatalytic efficiency upto four cycles, which supported the reusability of the Cd-MOF catalyst. Moreover, the PXRD patterns of Cd-MOF before and after dye degradation experiments resembled each other (with a slight change in intensity of peaks) (Fig S27 a and b) which indicated that Cd-MOF retained its crystalline nature after the photocatalytic activity.

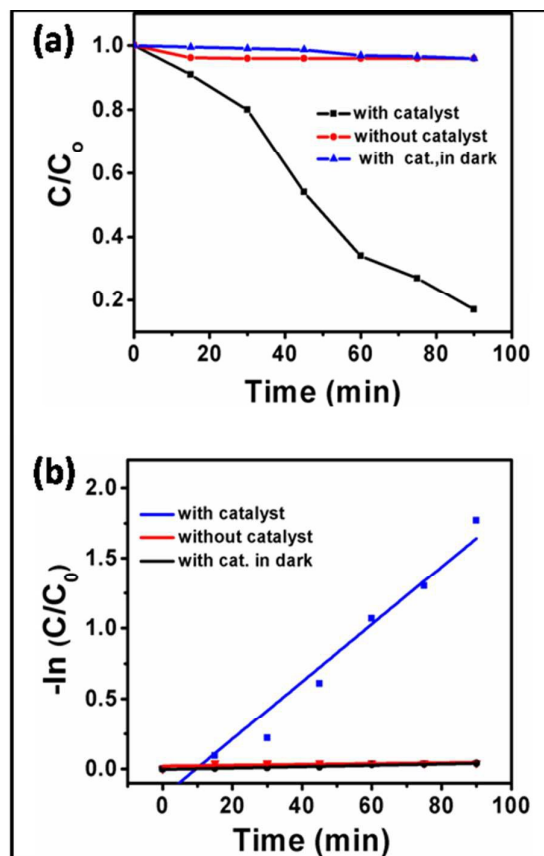


**Fig. 7** (a) Kinetic curves for photocatalytic degradation of MB. (b) Pseudo-first order kinetics plot for photocatalytic degradation of MB.

constant in the absence of Cd-MOF catalyst (Fig. 6c). This clearly indicated the negligible self-photosensitization of MB. The degradation experiment in dark was performed to confirm whether the dye was actually degraded or simply undergo adsorption by Cd-MOF (Fig. 6d). As the degradation was almost negligible in the dark,

## Mechanism for the degradation of MB

It is well known that hydroxyl radical plays key role for the degradation process due to its strong oxidizing power which is able to oxidize wide variety of double bonds containing organic compounds.<sup>10,43</sup> So, photocatalytic efficiency depends on the generation of hydroxyl radicals by photocatalyst. Consequently, to describe the photo degradation process the HOMO-LUMO gap can be utilized (Fig. 9). In general, the HOMO is mainly contributed by N

## PAPER

## Dalton Trans.

and O bonding electrons and LUMO is contributed by transition metals. Upon irradiation, the electrons in the HOMO of Cd-MOF got

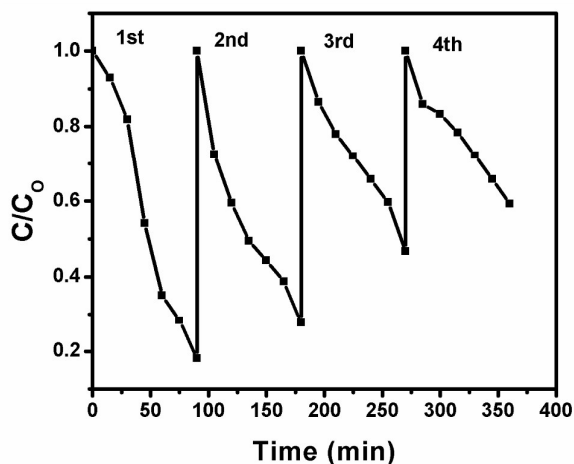


**Fig. 8** Reusability test of Cd-MOF upto four cycles for the photocatalytic degradation of MB dye.

excited and transferred to LUMO, leads to produce holes ( $h^+$ ) in the HOMO. These holes having high oxidizing ability either oxidize water molecules or react with hydroxyl ions to form hydroxyl radicals. These OH radical could be responsible to furnish the photodegradation process.<sup>44,45</sup>

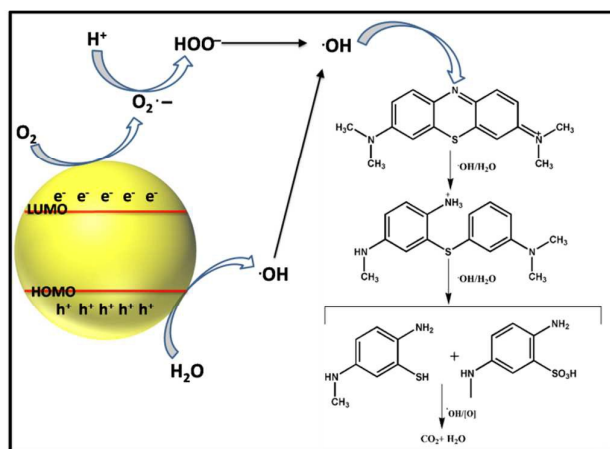


**Fig. 9** Mechanism proposed for the photodegradation of MB under visible light irradiation.

At the same time, molecular oxygen ( $O_2$ ) captures photogenerated electrons ( $e^-$ ) to produce superoxide radicals ( $O_2^{\cdot-}$ ) which also possess strong oxidizing ability and hence decompose the organic molecule (MB) into  $CO_2$ ,  $H_2O$  and some other degradation products. The foremost advantages of this photocatalyst are its high crystalline nature and large surface area which are responsible for the enhanced photocatalytic performance as these provide strong adsorption ability and result into adsorption of large number of pollutant molecules on catalyst surface.

The degradation of the dye was further confirmed by the LC-MS analysis of the degraded aqueous solution of methylene blue. The mechanistic pathway (Fig. S31) has been proposed for the degradation of MB by Cd-MOF. First of all, the hydroxyl radical attacks the ring containing both the heteroatoms N and S which results into opening of the central aromatic ring. Further the C-S bond breaks and it results into formation of fragments like 2-amino-5-(methylamino)-hydroxybenzenesulphonic acid and 2-amino-5-(N-methylformamido)-benzenesulphonic acid which were confirmed by LC-MS peaks at 218 and 230. These fragments got decomposed into smaller molecules like 2-amino-5-(methylamino)benzenethiol, 2-amino-5-(methylamino)benzenesulphonic acid and 2-aminophenol that corresponds to peaks at 154, 202.9 and 109 (Fig. S32-S34). At the end all these intermediates will get decomposed into  $CO_2$  and  $H_2O$ .

## Conclusions

In summary, we report the development of an integrated new catalytic platform through incorporation of iodine into a porous Cd-MOF being peripheral amine functionality and performed catalysis for the various important organic transformations. Especially in case of benzimidazole synthesis,  $I_2@Cd-MOF$  showed exceptional performance at mild reaction conditions and in a short span of time (6h). In contrast, the same reaction in the presence of molecular  $I_2$  requires high reaction temperature and longer reaction time for completion. Apart from this, thienyldipyrromethane transformation also established the good efficiency and reusability of this MOF. Thus, the detailed study of organic catalysis using  $I_2@Cd-MOF$  reflects its good catalytic efficiency for clean organic transformations. Further, the pristine Cd-MOF was investigated to evaluate its potential to act as photocatalyst for dye degradation under visible light illumination. Interestingly owing to its low band gap and strong visible light absorption properties, the MOF was evaluated to be efficient catalyst for photoinduced dye degradation without the use of additional oxidizer. The efficiency was evaluated to be 82% degradation of MB dye which is much higher than many reported catalytic systems. These studies provide an insight into the synthesis and applications of multifunctional MOFs.

## Conflicts of interest

There are no conflicts to declare.

## Acknowledgements

Financial support received from DST-SERB, India (IITM/SERB/RRK/173) and IIT Mandi (IITM/SG/NRT-58) are thankfully acknowledged. M. V. thanks CSIR for the fellowship. We thank Director, IIT Mandi for research facilities. The support of Advanced Materials Research Centre (AMRC), IIT Mandi, for sophisticated instrument facility is thankfully acknowledged.

## Notes and references:

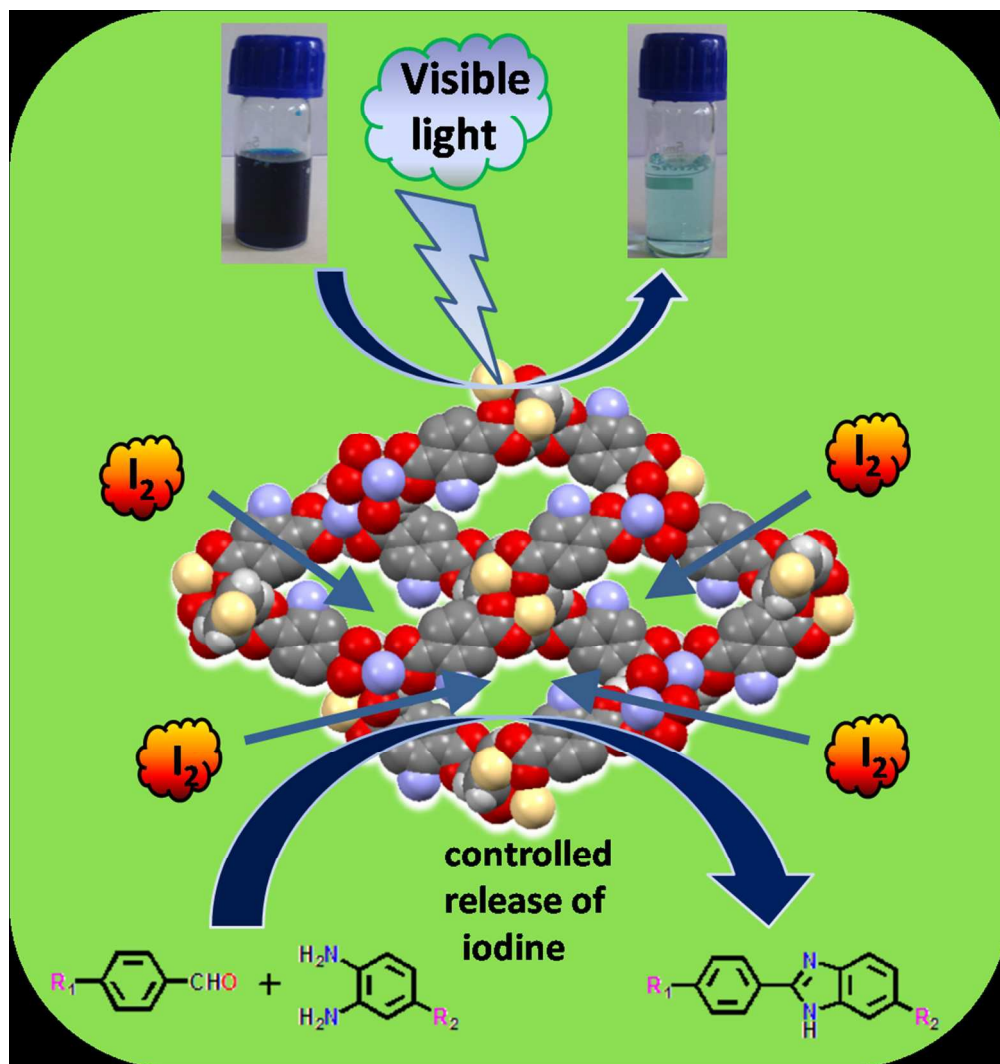
- 1 (a) L. Ma, C. Abney, W. Lin, *Chem. Soc. Rev.*, 2009, **38**, 1248-1256; (b) Y. B. Huang, J. Liang, X. S. Wang, R. Cao, *Chem. Soc. Rev.*, 2017, **46**, 126; (c) M. Allendorf, C. Bauer, R. Bhakta, R. Houk, *Chem. Soc. Rev.*, 2009, **38**, 1330-1352.
- 2 (a) S. Biswas, T. Ahnfeldt, N. Stock, *Inorg. Chem.*, 2011, **50**, 9518-9526; (b) Y.-L. Li, Y. Zhao, P. Wang, Y.-S. Kang, Q. Liu, X.-D. Zhang, W.-Y. Sun, *Inorg. Chem.*, 2016, **55**, 11821-11830.
- 3 K. Li, D. H. Olson, J. Y. Lee, W. Bi, K. Wu, T. Yuen, Q. Xu, J. Li, *Adv. Funct. Mater.*, 2008, **18**, 2205-2214.
- 4 M. Venkateswarulu, A. Pramanik, R.R. Koner, *Dalton Trans.*, 2015, **44**, 6348.
- 5 (a) H.-L. Jiang, Y. Tatsu, Z.-H. Lu, Q. Xu, *J. Am. Chem. Soc.*, 2010, **132**, 5586-5587; (b) R. Q. Zou, H. Sakurai, S. Han, R. Q. Zhong, Q. Xu, *J. Am. Chem. Soc.*, 2007, **129**(27), 8402-8403.
- 6 Y. L. Li, Y. Zhao, Y. S. Kang, X. H. Liu, W. Y. Sun, *Cryst. Growth Des.*, 2016, **16**, 7112-7123.
- 7 H.-L. Jiang, Q. Xu, *Chem. Commun.*, 2011, **47**, 3351-3370.
- 8 Y. Cui, B. Li, H. He, W. Zhou, B. Chen, G. Qian, *Acc. Chem. Res.*, 2016, **49**, 483-493.
- 9 (a) I.H. Hwang, J.M. Bae, W.S. Kim, Y.D. Jo, C.Kim, Y. Kim, S.J. Kim, S.Huh, *Dalton Trans.*, 2012, **41**, 12759-12765; (b) A. Dhakshinamoorthy, M. Alvaro, A. Corma, H. Garcia, *Dalton Trans.*, 2011, **40**, 6344.
- 10 A. Majedi, F. Davar, A. Abbasi, *Int. J. Nano Dimens.*, 2016, **7**, 1.
- 11 R. P. Antony, A.K. Satpati, K. Bhattacharyya, B. N. Jagatap, *Adv. Mater. Interfaces*, 2016, **1600632**.
- 12 (a) P. V. Dau, S. M. Cohen, *Chem. Commun.*, 2013, **49**, 6128; (b) A. Dhakshinamoorthy, A. M. Asiri, H. Garcia, *Chem. Commun.*, 2017, **53**, 10851.
- 13 S. Qiu, G. Zhu, *Coor. Chem. Rev.*, 2009, **253**, 2891-2911.
- 14 (a) N.-X. Zhu, C.-W. Zhao, J.-C. Wang, Y.-A. Li, Y.-B. Dong, *Chem. Commun.*, 2016, **52**, 12702-12705; (b) P. Rangaraj, S. Parshamoni, S. Konar, *Chem. Commun.*, 2015, **51**, 15526-15529.
- 15 X.-M. Zhang, C.-W. Zhao, J.-P. Ma, Y. Yu, Q.-K. Liu, Y.-B. Dong, *Chem. Commun.*, 2015, **51**, 839-842.
- 16 G. Yadav, S. Ganguly, *Eur. J. Med. Chem.*, 2015, **97**, 419-443.
- 17 A. Figge, H. J. Altenbach, D. J. Brauer, P. Tielmann, *Tetrahedron: Asymmetry*, 2002, **13**, 137-144.
- 18 H. Barker, R. Smyth, H. Weissbach, J. Toohey, J. Ladd, B. Volcani, *J. Bio. Chem.*, 1960, **235**, 480-488.
- 19 O. Ravi, A. Shaikh, A. Upare, K. K. Singarapu, S. R. Bathula, *J. Org. Chem.*, 2017, **82**, 4422-4428.
- 20 J. Bartelmess, E. De Luca, A. Signorelli, M. Baldrighi, M. Becce, R. Brescia, V. Nardone, E. Parisini, L. Echegoyen, P. P. Pompa, *Nanoscale* 2014, **6**, 13761-13769.
- 21 L.-Y. Niu, Y.-S. Guan, Y.-Z. Chen, L.-Z. Wu, C.-H. Tung, Q.-Z. Yang, *J. Am. Chem. Soc.*, 2012, **134**, 18928-18931.
- 22 R. K. Totten, Y.-S. Kim, M. H. Weston, O. K. Farha, J. T. Hupp, S. T. Nguyen, *J. Am. Chem. Soc.*, 2013, **135**, 11720-11723.
- 23 C.-C. Wang, J.-R. Li, X.-L. Lv, Y.-Q. Zhang, G. Guo, *Energy Environ. Sci.*, 2014, **7**, 2831-2867.
- 24 H.-P. Jing, C.-C. Wang, Y.-W. Zhang, P. Wang, R. Li, *RSC Adv.*, 2014, **4**, 54454-54462.
- 25 S. Parshamoni, S. Sanda, H. S. Jena, S. Konar, *Chem. Asian J.*, 2015, **10**, 653-660.
- 26 S. Kumar, V. Sharma, K. Bhattacharyya, V. Krishnan, *New J. Chem.*, 2016, **40**, 5185-5197.
- 27 P. Saxena, N. Thirupathi, *Poly.*, 2015, **06**, 002.
- 28 M. Ishihara, H. Togo, *Synlett* 2006, **2006**, 227-230.
- 29 S. K. Wang, M. T. Chen, D. Y. Zhao, X. You, Q. L. Luo, *Adv. Synth. Catal.*, 2016, **358**, 4093-4099.
- 30 N. Tada, M. Shomura, L. Cui, T. Nobuta, T. Miura, A. Itoh, *Synlett*, 2011, **2011**, 2896-2900.
- 31 C. Falaise, C. Volkringer, J. Facqueur, T. Bousquet, L. Gasnot, T. Loiseau, *Chem. Commun.*, 2013, **49**, 10320-10322.
- 32 B. Xin, G. Zeng, L. Gao, Y. Li, S. Xing, J. Hua, G. Li, Z. Shi, S. Feng, *Dalton Trans.*, 2013, **42**, 7562-7568.
- 33 P. Mahata, G. Madras, S. Natarajan, *J. Phys. Chem. B*, 2006, **110**, 13759-13768.
- 34 Y. Gong, T. Wu, J. Lin, *CrystEngComm*, 2012, **14**, 3727-3736.
- 35 J. K. Vaishnav, S. S. Arbuji, S. B. Rane, D. P. Amalnerkar, *RSC Adv.*, 2014, **4**, 47637-47642.
- 36 Y. Liu, S. Xie, H. Li, X. Wang, *ChemCatChem*, 2014, **6**, 2522-2526.
- 37 M. Saranya, R. Ramachandran, P. Kollu, S. K. Jeong, A. N. Grace, *RSC Adv.*, 2015, **5**, 15831-15840.
- 38 C.-B. Liu, H.-Y. Sun, X.-Y. Li, H.-Y. Bai, Y. Cong, A. Ren, G.-B. Che, *Inorg. Chem. Commun.*, 2014, **47**, 80-83.
- 39 C.-B. Liu, Y. Cong, H.-Y. Sun, G.-B. Che, *Inorg. Chem. Commun.*, 2014, **47**, 71-74.
- 40 H.-Y. Sun, C.-B. Liu, Y. Cong, M.-H. Yu, H.-Y. Bai, G.-B. Che, *Inorg. Chem. Commun.*, 2013, **35**, 130-134.
- 41 X. Wang, J. Luan, H. Lin, C. Xu, G. Liu, J. Zhang, A. Tian, *CrystEngComm* 2013, **15**, 9995-10006.
- 42 X. Wang, J. Luan, H. Lin, Q. Lu, C. Xu, G. Liu, *Dalton Trans.*, 2013, **42**, 8375-8386.
- 43 S. Xia, L. Zhang, G. Pan, P. Qian, Z. Ni, *Phys. Chem. Chem. Phys.*, 2015, **17**, 5345-5351.
- 44 J.-J. Du, Y.-P. Yuan, J.-X. Sun, F.-M. Peng, X. Jiang, L.-G. Qiu, A.-J. Xie, Y.-H. Shen, J.-F. Zhu, *J. Hazard. Mater.*, 2011, **190**, 945-951.
- 45 X. Chen, F. Zhang, Q. Wang, X. Han, X. Li, J. Liu, H. Lin, F. Qu, *Dalton Trans.*, 2015, **44**, 3034-3042.

PAPER

Dalton Trans.

Dalton Transactions Accepted Manuscript

Published on 13 December 2017. Downloaded by Fudan University on 13/12/2017 10:34:48.



180x190mm (150 x 150 DPI)